

Pressure-induced formation of intermediate-valence quasicrystalline system in a Cd-Mg-Yb alloyTetsu Watanuki,^{1,*} Daichi Kawana,^{1,†} Akihiko Machida,¹ and AnPang Tsai²¹Condensed Matter Science Division, Japan Atomic Energy Agency, Sayo, Hyogo 679-5148, Japan²Institute of Multidisciplinary Research for Advanced Material, Tohoku University, Sendai 980-8577, Japan

(Received 27 April 2011; revised manuscript received 6 July 2011; published 15 August 2011)

A quasiperiodic intermediate-valence system was prepared by applying pressure to an icosahedral Cd-Mg-Yb quasicrystal. X-ray absorption spectroscopy near the Yb L_3 edge demonstrates that the Yb valence increases continuously upon compression from the divalent state ($4f^{14}$) at ambient pressure and reaches a value of 2.71 at 57.6 GPa, which is close to the trivalent state ($4f^{13}$). By following the trend of Yb-based intermediate-valence crystalline compounds, this large valence increase suggests the change of $4f$ character in the Cd-Mg-Yb quasicrystal from an itinerant state with weak electron correlations to an intermediate region between an itinerant and a localized state with strong correlations. The valence increases sensitively with pressure below ~ 30 GPa; however, the increase is significantly suppressed above ~ 30 GPa. The rate of valence increase with respect to pressure in the lower-pressure region is twice larger than that of a Cd-Yb quasicrystal in our previous study [Phys. Rev. B **81**, 220202(R) (2010)]. This is mainly explained by the smaller bulk modulus of the Cd-Mg-Yb quasicrystal compared to the Cd-Yb system. The suppression of valence increase with respect to pressure in the higher-pressure region is most likely due to an increase of conduction- $4f$ electron hybridization that counteracts $4f$ localization and reduces the Yb valence increase.

DOI: 10.1103/PhysRevB.84.054207

PACS number(s): 71.23.Ft, 71.28.+d, 78.70.Dm

I. INTRODUCTION

Recently, we have demonstrated quasiperiodic, intermediate-valence (IV) systems by applying pressure to Yb-based quasicrystals.^{1,2} Yb ions show a divalent form in $\text{Cd}_{84}\text{Yb}_{16}$ and $\text{Cd}_{23}\text{Mg}_{61}\text{Yb}_{16}$ icosahedral quasicrystals ($i\text{-CdYb}$ and $i\text{-CdMgYb}$, respectively),^{3,4} similar to other known Yb-based quasicrystalline alloys.^{5,6} However, Yb L_3 -edge x-ray absorption spectroscopy demonstrates that Yb valence increases upon compression, and Yb ions assume noninteger valence states. Both $i\text{-CdYb}$ and $i\text{-CdMgYb}$ consist of Tsai-type atomic clusters in which 12 Yb ions form an icosahedron as the third shell of the cluster (Fig. 1).⁷ The 12 Yb icosahedra are arranged according to a τ^3 -scaling inflation rule, where τ is the golden mean,^{7,8} and form a quasiperiodic lattice of IV Yb ions between divalent ($4f^{14}$) and trivalent ($4f^{13}$) states.

Yb-based IV crystalline compounds show diverse physical properties depending on the valence of Yb. An increase in valence corresponds to an increase in the $4f$ -hole density due to the relation $\nu = n_h + 2$, where ν is the Yb valence, and n_h is the $4f$ -hole number per Yb site. This, in turn, implies that the $4f$ hole-hole correlation becomes stronger and the behavior of $4f$ holes changes from itinerant to more localized. Depending on the electron correlation effects, various phenomena have been observed in such systems, such as a valence fluctuation, heavy-fermion state, non-Fermi-liquid behavior, superconductivity, charge ordering, and complex magnetic ordering.⁹

What types of physical properties occur in Yb-based IV quasicrystals as Yb valence increases? In order to answer this question, it is necessary to extend the valence region from divalent at ambient pressure toward trivalent in IV quasicrystalline systems. A valence of 2.7 is desirable at the present stage, since it is the approximate value of the

boundary between itinerant and localized behavior of a $4f$ system in Yb-based IV crystalline compounds.^{2,10} In the lower valence region $\nu \lesssim 2.7$ ($n_h \lesssim 0.7$), these compounds show a rather low electronic specific-heat coefficient (γ) below $\sim 10^2$ mJ/mol K², indicating a valence fluctuation regime with itinerant $4f$ -hole motion due to weak electron correlations. In the higher valence region of $\nu \gtrsim 2.7$ ($n_h \gtrsim 0.7$), γ exceeds $\sim 10^2$ mJ/mol K², and the $4f$ holes are localized or behave as heavy fermions at low temperature due to strong electron correlations.

Our previous studies have shown that Yb valence in $i\text{-CdYb}$ and $i\text{-CdMgYb}$ increases nearly linearly upon compression and reaches 2.33 at 31.7 GPa and 2.37 at 16.3 GPa for the two alloys, respectively.^{1,2} The valence increase upon compression is attributed to the properties of the Yb ion; the ionic radius decreases as divalent Yb shifts to the trivalent state. Therefore, a larger pressure effect on the valence increase is expected for the more compressible quasicrystal. It is possible to substitute Mg, a small bulk modulus element, at Cd sites in $i\text{-CdYb}$.^{4,11} The Mg-substituted alloys of $\text{Cd}_{84-x}\text{Mg}_x\text{Yb}_{16}$ form stable quasicrystals in a wide composition range of $x = 0\text{--}61$ at.% Mg, and $i\text{-CdMgYb}$ is found at the upper substitution limit. Hence $i\text{-CdMgYb}$ is expected to be the most compressible of these alloys and to demonstrate the largest pressure effect on the valence increase among the $\text{Cd}_{84-x}\text{Mg}_x\text{Yb}_{16}$ quasicrystals. In our previous study,² limited to a low-pressure region, $i\text{-CdMgYb}$ indeed exhibited a larger pressure effect than $i\text{-CdYb}$.

In this paper, we apply further pressure to $i\text{-CdMgYb}$ up to 57.6 GPa and succeed in extending the Yb valence region up to 2.71. While the valence increases sensitively with pressure in the lower-pressure region, the change in valence is significantly suppressed above ~ 30 GPa. Below we also discuss the mechanism of such pressure dependence.

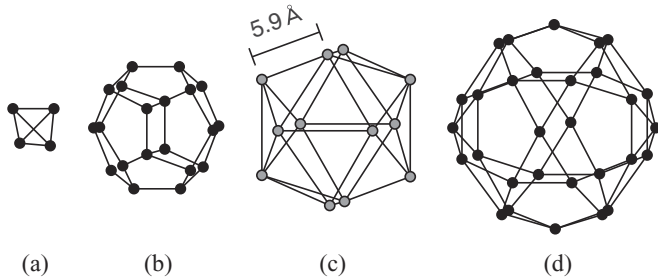


FIG. 1. Successive shells of the Tsai-type atomic cluster in a $\text{Cd}_{84}\text{Yb}_{16}$ icosahedral quasicrystal ($i\text{-CdYb}$): (a) 4Cd tetrahedron, (b) 20Cd dodecahedron, (c) 12Yb icosahedron, and (d) 30Cd icosidodecahedron. A $\text{Cd}_{23}\text{Mg}_{61}\text{Yb}_{16}$ icosahedral quasicrystal ($i\text{-CdMgYb}$) is obtained by Mg substitution at the Cd sites.

II. EXPERIMENT

The Yb valence of $i\text{-CdMgYb}$ under pressure was measured by x-ray absorption near edge structure (XANES) experiments. An alloy with nominal composition of $\text{Cd}_{24}\text{Mg}_{60}\text{Yb}_{16}$ was prepared from high-purity elements of Cd (purity, 99.99 wt%), Mg (purity, 99.99 wt%), and Yb (purity, 99.9 wt%) in a sealed steel tube in an electric furnace under argon atmosphere. The alloy was first melted at 1123 K and then kept at 963 K for 1 h. Subsequently it was cooled down to 873 K over 100 h, followed by a water quenching. The resultant quasicrystal was analyzed to have a composition of $\text{Cd}_{23}\text{Mg}_{61}\text{Yb}_{16}$ by an electron probe microanalyzer (EPMA). The formation of a single quasicrystalline phase was confirmed by an x-ray diffraction measurement using Cu $K\alpha$ radiation. A cracked $40\ \mu\text{m} \times 30\ \mu\text{m} \times 10\ \mu\text{m}$ piece of the alloy was sealed in a diamond anvil cell (DAC) with a pressure medium of 4:1 methanol-ethanol and a ruby-chip pressure marker. Yb L_3 -edge XANES experiments were performed under pressures up to 57.6 GPa at room temperature in BL22XU at SPring-8. The $20\ \mu\text{m}$ -diam collimated monochromatic x-ray beam was directed at the center of the sample. Transmission XANES spectra were acquired by scanning the incident x-ray energy between 8.77 and 9.11 keV using two ionization chambers filled with N_2 gas to monitor the incident and transmitted x-ray intensities. The x-ray energy was calibrated by measuring K -edge absorption spectra of a Cu foil. In order to determine the volume compression upon applying pressure, x-ray diffraction measurements were performed in the same compression sequence. The incident x-ray energy was tuned to 9.04 keV and diffraction signals were acquired within the 2θ angle of 20.5° by switching the detector from the ionization chamber (monitoring transmitted x rays) to the imaging plate system of the diffractometer for DAC in BL22XU.¹² Under these conditions, the detection area of the diffraction profiles was limited to a small q range within $1.63\ \text{\AA}^{-1}$. Nevertheless, the d -value shifts upon compression were detectable.

III. RESULTS

Figure 2 shows the normalized XANES spectra of $i\text{-CdMgYb}$ at select pressures. At ambient pressure, a single divalent absorption peak is observed at 8.940 keV [Fig. 2(a)].

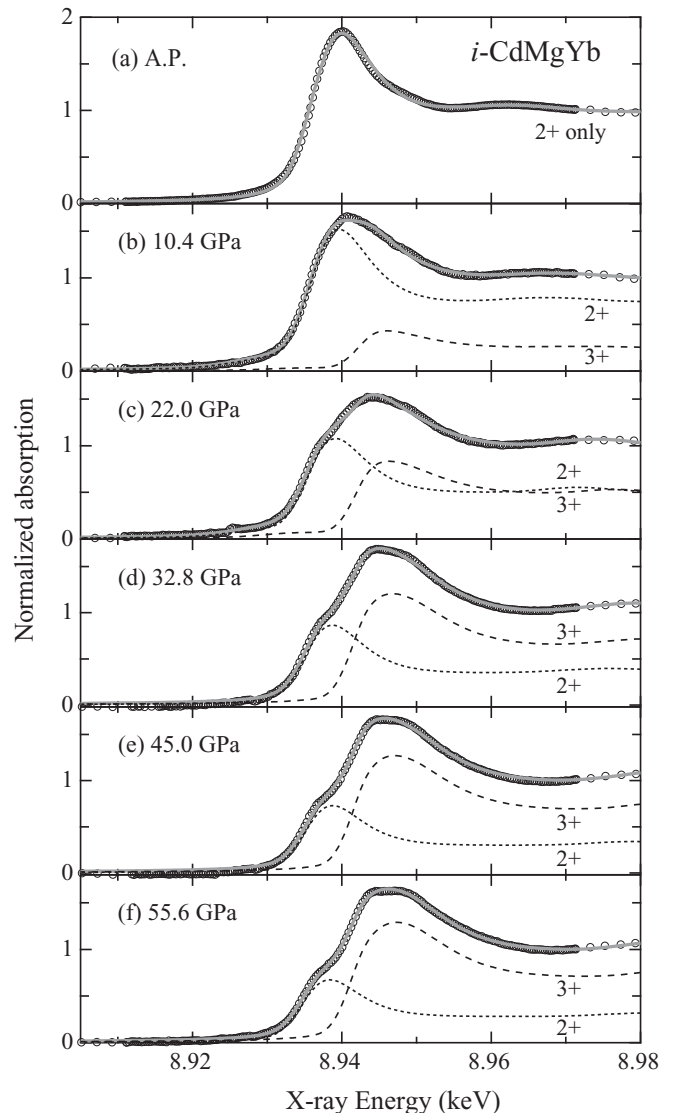


FIG. 2. Normalized Yb L_3 XANES spectra of $\text{Cd}_{23}\text{Mg}_{61}\text{Yb}_{16}$ icosahedral quasicrystal ($i\text{-CdMgYb}$) at select pressures at room temperature (open circles). Background absorption is removed via Victoreen's formula adjusted to the lower-energy data between 8.77 and 8.90 keV (not shown). Normalization is then applied so that the higher-energy data up to 9.11 keV asymptotically approaches a unit. Each spectrum is fitted by the sum (gray line) of the divalent (dotted line) and trivalent (dashed line) components.

Upon compression the divalent peak decreases and a trivalent component appears at ~ 8.946 keV, as in our previous report of Ref. 2. The trivalent component rises constantly with increasing pressure below ~ 30 GPa [Figs. 2(a)–2(d)]. In the higher-pressure region, however, the change in the spectrum is reduced and finally disappears as in Figs. 2(d)–2(f). The trivalent component shows a trapezoidlike peak as seen in the higher-pressure region. The peak center position is ~ 8.946 keV, which is 6 eV higher than the divalent one and is the appropriate value for the trivalent component. Such a complex peak structure of a trivalent component with slight splitting has been observed in other Yb-based IV materials, for example, YbInCu_4 .¹³ In Fig. 2, the profile at the second

highest pressure is given due to lack of fine energy resolution data at the highest pressure.

The mean valence at each pressure was determined using a procedure similar to the one in our previous report of Ref. 1. The divalent component profile $S_{div}(E)$ was expressed as a combination of an asymmetric Gaussian and an arctangent function that well reproduced the spectrum profile at ambient pressure [Fig. 2(a)]. Unlike in the previous paper, the same function with an energy shift of $S_{div}(E - \Delta)$ should not be applied for the trivalent component profile $S_{tri}(E)$, since the peak shape is different from the divalent one. Here $S_{tri}(E)$ was obtained by subtracting $\alpha S_{div}(E)$ (α is a constant) from the observed spectrum at 32.8 GPa [Fig. 2(d)]. The value of α was tuned so that the remaining spectrum showed an appropriate profile in which the edge and the peak shape were smoothly connected. The residual spectrum was then expressed as a combination of the peak part of two asymmetric Gaussians and the step part of an arctangent function. Here the ratio of the integrated peak intensity to the step height of the arctangent function was fixed to be the same as that of $S_{div}(E)$. As shown in Fig. 2, the spectrum at each pressure was well fitted by the sum of the divalent and trivalent components $(1 - x)S_{div}(E) + xS_{tri}(E)$. The mean valence was obtained from $\bar{v} = x + 2$.

Figure 3 shows the pressure dependence of the mean valence. The valence increases nearly linearly and reaches 2.63 at 30.7 GPa. The pressure effect on the valence increase is obviously larger than that of i -CdYb. The rate of valence change with respect to pressure below 25 GPa, $dv/dP_{i-CdMgYb} = 0.022 \text{ GPa}^{-1}$, is twice that of i -CdYb, $dv/dP_{i-CdYb} = 0.011 \text{ GPa}^{-1}$. However, this rate is significantly reduced above 30 GPa in accordance with the observation of the spectrum change. Subsequently, the valence nearly plateaus above 45 GPa and is 2.71 at 57.6 GPa. In order to check the absolute value of the valence, we have analyzed the

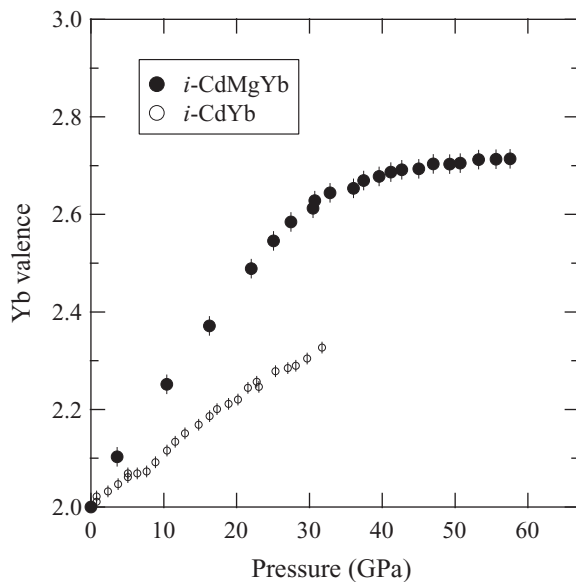
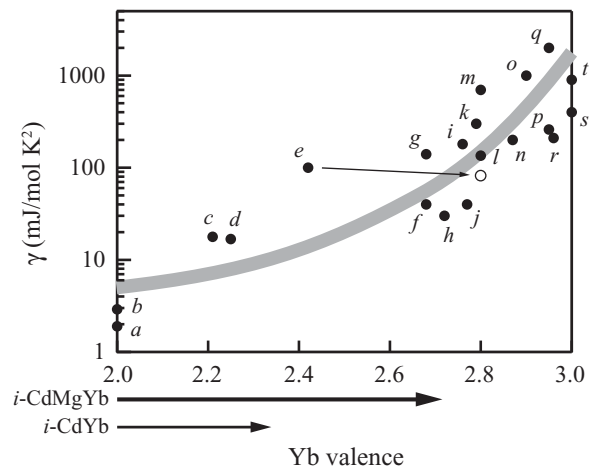


FIG. 3. Pressure dependence of Yb valence in a $\text{Cd}_{23}\text{Mg}_{61}\text{Yb}_{16}$ icosahedral quasicrystal, i -CdMgYb (closed circles). Results of our previous study on a $\text{Cd}_{84}\text{Yb}_{16}$ icosahedral quasicrystal, i -CdYb, are also shown (open circles, Ref. 1).



- a) YbPb₃ f) YbInAu₂ k) YbFe₄P₁₂ p) YbCuAl
- b) Yb g) YbFe₄Sb₁₂ l) YbCu₂Si₂ q) YbAuCu₄
- c) Yb₂Pd₃Sn₅ h) YbTiCu₄ m) Yb₂Ni₂Al r) YbInCu₄
- d) YbAl₂ i) YbCdCu₄ n) YbAgCu₄ s) Yb₂Fe₃Si₅
- e) Yb₂Pt₃Sn₅ j) YbAl₃ o) YbRh₂Si₂ t) YbSi

FIG. 4. Yb valence region developed in this study on a $\text{Cd}_{23}\text{Mg}_{61}\text{Yb}_{16}$ icosahedral quasicrystal (i -CdMgYb) as well as that in the previous work on $\text{Cd}_{84}\text{Yb}_{16}$ icosahedral quasicrystal (i -CdYb) in Ref. 1. For comparing with the trend of intermediate-valence Yb-based crystalline compounds, the relationship between the electronic specific heat coefficient (γ) and the Yb valence in these compounds is shown. The open circle denotes the contribution of the higher valence ions in $\text{Yb}_2\text{Pt}_3\text{Sn}_5$. More detailed information regarding this plot is given in Ref. 2.

spectrum at 55.6 GPa with the valence of 2.71 [Fig. 2(f)] by describing the $S_{tri}(E)$ peak shape as a single asymmetric Gaussian. Profile fitting was performed with setting the peak width at several possible values. In spite of the oversimplified peak expression, the valence was calculated to be between 2.70 and 2.77, which proves the reliability of the above analysis.

We have thus succeeded in extending the Yb valence region from the divalent at ambient pressure to the target value of 2.7 as shown in Fig. 4, although the valence increase was suppressed in the higher-pressure region. Following the trend of Yb-based IV crystalline compounds, this valence change suggests that the $4f$ system in i -CdMgYb varies from a valence fluctuation regime of itinerant $4f$ holes with weak electron correlations to the boundary of the Kondo regime with nearly localized $4f$ holes due to strong electron correlations.

Figure 5(a) shows the volume compression curve of i -CdMgYb determined by the d -value measurements of the x-ray diffraction analysis. The normalized d values d/d_0 (d_0 is the d value at ambient pressure) of several reflections were acquired at each pressure. The normalized volume V/V_0 was calculated as the cube of the average d/d_0 , $V/V_0 = (d/d_0)^3$. The volume compression curve shows a monotonic decrease. It is found that the volume of i -CdMgYb is obviously more compressible than that of i -CdYb, as expected from the Mg substitution. The bulk modulus was derived by fitting a Birch-Murnaghan equation of state as shown below to

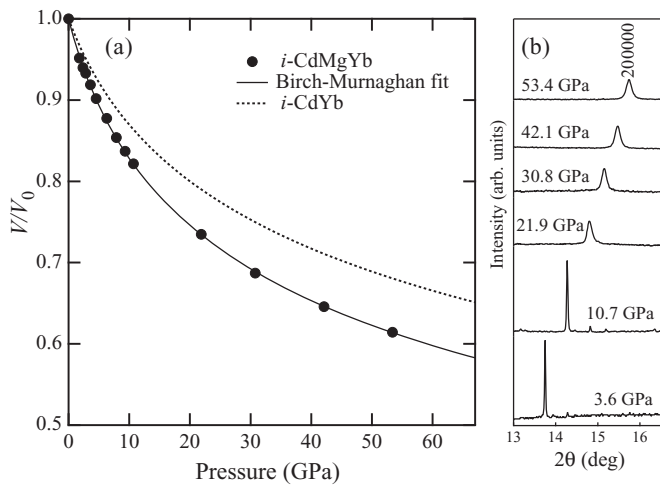


FIG. 5. (a) The pressure-volume relationship of a $\text{Cd}_{23}\text{Mg}_{61}\text{Yb}_{16}$ icosahedral quasicrystal (i -CdMgYb, closed circles). The solid line shows a fit of the Birch-Murnaghan equation of state. Compression curve of a $\text{Cd}_{84}\text{Yb}_{16}$ icosahedral quasicrystal (i -CdYb) is also shown (dotted line, Ref. 14). (b) Bragg peak profile of 200000 reflection at select pressures.

the volume compression curve, $B_0^{i\text{-CdMgYb}} = 33.9(4)$ GPa, $B_0^{i\text{-CdMgYb}} = 4.7(1)$:

$$P = \frac{3}{2}B_0[(V/V_0)^{-\frac{2}{3}} - (V/V_0)^{-\frac{5}{3}}] \times \left\{1 + \frac{3}{4}(B_0' - 4)[(V/V_0)^{-\frac{2}{3}} - 1]\right\}. \quad (1)$$

The B_0 value is approximately two thirds of $B_0^{i\text{-CdYb}} = 49.2$ GPa.¹⁴ In addition, the value is remarkably lower than the reported typical ones above 100 GPa for quasicrystalline alloys.¹⁵

Figure 5(b) shows the Bragg peak profile of the 200000 reflection along the fivefold axis at select pressures. A distinct peak broadening with increasing pressure from 10.7 to 21.9 GPa is observed, as well as other reflections. This broadening is caused by a nonhydrostatic compression due to the solidification of the pressure medium. The pressure deviation ΔP is estimated to be ± 1.4 GPa at 21.9 GPa from the Bragg peak width $\Delta 2\theta$ on the assumption of $\Delta P = dP/d(2\theta)\Delta 2\theta$. In spite of the apparent peak broadening, no anomaly is found in the pressure dependence of Yb valence in this pressure range (Fig. 3) as well as in the volume compression curve. Therefore, the influence of the nonhydrostatic compression on the valence measurement is judged to be negligible.

Figure 6 shows a plot of the valence change versus volume compression obtained by combining valence- and volume-change data as a function of pressure. With decreasing volume, the valence increase accelerates in the lower compression region of $0.7 \lesssim V/V_0 \leq 1$ ($P \lesssim 30$ GPa). However, the valence change significantly decelerates in the high compression region of $V/V_0 \lesssim 0.7$ ($P \gtrsim 30$ GPa), and finally the valence nearly plateaus. Thus, the suppression of valence increase is observed not only in the pressure dependence but also as a function of volume decrease. These results indicate that the

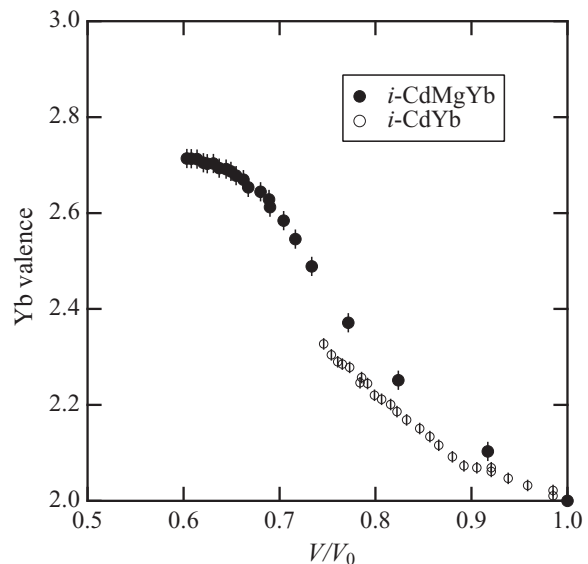


FIG. 6. Yb valence as a function of volume compression in a $\text{Cd}_{23}\text{Mg}_{61}\text{Yb}_{16}$ icosahedral quasicrystal, i -CdMgYb (closed circles) and in a $\text{Cd}_{84}\text{Yb}_{16}$ icosahedral quasicrystal, i -CdYb (open circles).

valence saturation behavior upon applying pressure (Fig. 3) is not due to a decreasing of volume compression ratio dV/dP at high pressures, which is the typical reason for pressure effects reducing at high pressures. The results point out that the Yb ionic radius does not decrease even with a volume decrease, and the scheme of increasing valence by applying pressure does not work intrinsically for higher pressures.

IV. DISCUSSION

The Yb valence region of i -CdMgYb has been extended to the target value of 2.7. This achievement is mainly due to the valence increase being more sensitive to pressure compared with i -CdYb. Below we examine the role of Mg substitution in the observed large-pressure effect on valence. In addition, we find that the valence increase did not proceed simply with increasing pressure but was significantly suppressed and finally reached a plateau in the higher-pressure region. We also investigate the mechanism of this valence increase suppression.

Mg substitution resulted in a decrease in the bulk modulus, as expected. The $B_0^{i\text{-CdMgYb}}$ value of 33.9 GPa is well explained by the composition-weighted average of the bulk moduli of each constituent element, $B_0^{\text{pure-Cd}} = 49.8$ GPa,¹⁶ $B_0^{\text{pure-Mg}} = 34.1$ GPa,¹⁶ and $B_0^{\text{pure-Yb}} = 14.6$ GPa.¹⁶ The composition-weighted average is 34.6 GPa, which is very close to the $B_0^{i\text{-CdMgYb}}$ value. For i -CdYb, the value of 49.2 GPa is also close to the composition-weighted average, 44.2 GPa. Therefore, we conclude that the bulk modulus decrease from $B_0^{i\text{-CdYb}}$ to $B_0^{i\text{-CdMgYb}}$ is due to the substitution of a more compressible element, as expected, and the degree of decrease is appropriate to the amount of Mg substitution.

Because i -CdMgYb is isostructural to i -CdYb, it is thought that the larger volume compression of the former causes larger

shrinkage of Yb site volume, corresponding to a larger valence shift toward the trivalent. In fact, the inverse ratio of the bulk moduli, $(B_0^{i\text{-CdMgYb}}/B_0^{i\text{-CdYb}})^{-1} = 1.45$, accounts for the main part of increase in the rate of change of valence with pressure $(dv/dP_{i\text{-CdMgYb}})/(dv/dP_{i\text{-CdYb}}) = 2.0$. This argument, however, assumes uniform contraction of the atomic arrangement under pressure. The remaining factor of $2.0/1.45 = 1.38$ should be due to the inaccuracy of this assumption. According to a theoretical prediction, dv/dP is inversely proportional to Yb concentration per volume.¹⁷ In the present case, $i\text{-CdMgYb}$ has a 6.6% larger isostructural unit volume than $i\text{-CdYb}$, which accounts for a further increase of dv/dP by a factor of 1.066. The remaining factor of $1.38/1.066 = 1.29$ might be attributed to nonuniform deformation, such as preferential shrinkage of the local structure around the Yb site, or else the difference between hybridization of Mg-Yb wave functions and that of Cd-Yb one, resulting in promoting the $4f$ electron delocalization from the Yb site. The former case may be caused by the site occupation preferences of Mg and Cd atoms.¹¹ The possibility of the latter case is implied in the XANES spectra. The observed complex structure of the trivalent peak for $i\text{-CdMgYb}$ is dissimilar to the simple one for $i\text{-CdYb}$.¹ The difference indicates that the Mg substitution induces a certain modification of the unoccupied Yb- $5d$ band, with an energy scale of several eV. One of the most likely candidates of this origin is the variation of the hybridization strength between the Yb wave function and that of surrounding atoms. The crystal field effect is another candidate, although it is less likely due to weak structural anisotropy of the Yb site surrounded by 16 atoms.^{7,8}

We have also investigated the mechanism of valence saturation behavior observed not only as a function of pressure but also volume decrease at the high-pressure, highly compressed region of $P \gtrsim 30$ GPa ($V/V_0 \lesssim 0.7$). The mechanism of stabilizing a smaller ionic radius upon compression should be effective as long as the volume decreases. If this mechanism only works, the valence will increase. Therefore, a counter mechanism has to arise in the high-pressure regime and suppress the valence increase even for volume compression.

As mentioned by Goltsev *et al.*,¹⁷ the counter mechanism is thought to be the increase of conduction (c)- f electron hybridization due to applied pressure. This mechanism has the effect of enhancing the itinerant character of $4f$ holes and consequently suppressing $4f$ -hole localization and reducing the Yb valence increase. Let us now briefly revisit the explanation in Ref. 17. The c - f hybridization due to the overlap between the wave functions of the $4f$ state and the conduction-band state grows exponentially with compressed volume. Hence, this mechanism is not effective when volume compression is small, but works well in the highly compressed regime. Therefore, in the high-pressure region this effect should compensate the valence increase which is due to the stabilization of the smaller ionic radius state. This compensation behavior is shown in Ref. 17 by calculating the Kondo temperature T_K and c - f exchange coupling J . These arguments are constructed regardless of the atomic arrangement and are applicable to quasicrystals. In this paper we have managed to observe the compensation behavior

in a quasiperiodic system by extending the range of pressures investigated. The volume compression ratio of $V/V_0 = 0.7$, which is the turning point for valence suppression, corresponds to a 10% decrease of interatomic distance. This value can be reasonably expected to cause a significant change in the c - f hybridization. Similar behavior has been shown in a report on YbAl_2 .^{13,18} The Yb valence increases nearly linearly from 2.25 at ambient pressure to 2.85 at 10 GPa. However, thereafter it shows a plateau with a value of 2.9 up to the maximum achieved pressure of 38.5 GPa, even though the volume should continue to decrease in this pressure range.¹⁹ For other Yb-based compounds and, moreover, for other divalent rare-earth-based compounds, such intrinsic suppression of the valence increase might also be observed in the high-pressure, highly compressed regime.

The electronic specific-heat coefficient γ of $i\text{-CdMgYb}$ is expected to increase upon compression. The value of γ should be comparable to that of $i\text{-CdYb}$ [2.87 mJ/mol K² (Ref. 20) or 1.1 mJ/mol K² (Refs. 21 and 22)] at ambient pressure and may exceed $\sim 10^2$ mJ/mol K² around the maximum valence of 2.71, as is typical for Yb-based IV crystalline compounds. Moreover, even larger γ is expected because electrons in quasicrystals tend to be localized.²³ A possibility of showing non-Fermi-liquid behavior also exists. On the one hand, for Yb-based IV crystalline compounds, the observation of non-Fermi-liquid behavior is limited to the neighborhood of a quantum critical point, where valence is close to trivalent, for example, 2.75 in the case of YbAlB_4 .^{9,24,25} On the other hand, the region of non-Fermi-liquid might be expanded for quasicrystalline systems because the k vector of the electron translational momentum is no longer a good quantum number. In the higher valence region, a charge disproportionation that corresponds to a quasiperiodic charge order or a charge glass is also possible due to increasing localization of $4f$ holes. A stable, charge-modulation state should appear in a constant valence region, and the observed valence plateau area in the high-pressure region readily meets this condition.

V. CONCLUSION

We have prepared a quasiperiodic IV system by applying pressure to $i\text{-CdMgYb}$ and have succeeded in extending the Yb valence region from the divalent at ambient pressure to a valence of 2.71 at 57.6 GPa as demonstrated in the XANES study. By following the trend of Yb-based IV crystalline compounds, this large valence change corresponds to the change of the $4f$ -hole character from an itinerant state with weak electron correlations to the boundary of the Kondo regime with a nearly localized state due to strong electron correlations.

The valence increases sensitively with pressure below ~ 30 GPa; however, the increase is significantly suppressed above ~ 30 GPa. The rate of valence increase as a function of pressure in the lower-pressure region is twice larger than that of $i\text{-CdYb}$, which is mainly because $i\text{-CdMgYb}$ is more compressible than $i\text{-CdYb}$. Due to the small bulk modulus of Mg, $i\text{-CdMgYb}$ has a smaller bulk modulus ($B_0 = 33.9$ GPa) than $i\text{-CdYb}$.

The suppression of the valence increase in the high-pressure region was observed not only as a function of pressure but also volume compression. This result can be explained by an increase of c - f electron hybridization that counteracts $4f$ localization and reduces the Yb valence increase.

ACKNOWLEDGMENTS

We thank M. Mizumaki for fruitful discussions and K. Kiriyama and H. Kaneko for their technical support. This work was performed under Proposals No. 2008B3701, No. 2009A3701, and No. 2009B3702 at BL22XU in SPring-8.

*wata@spring8.or.jp

[†]Present address: Condensed Matter Research Center, Institute of Materials Structure Science, KEK, Tsukuba 305-0801, Japan.

¹D. Kawana, T. Watanuki, A. Machida, T. Shobu, K. Aoki, and A. P. Tsai, *Phys. Rev. B* **81**, 220202(R) (2010).

²T. Watanuki, D. Kawana, A. Machida, and A. P. Tsai, *J. Phys. Soc. Jpn.* **80**(Suppl.A), SA087 (2011).

³A. P. Tsai, J. Q. Guo, E. Abe, H. Takakura, and T. J. Sato, *Nature (London)* **408**, 537 (2000).

⁴J. Q. Guo, E. Abe, and A. P. Tsai, *Philos. Mag. Lett.* **82**, 27 (2002).

⁵A. P. Tsai and C. P. Gómez, in *Quasicrystals*, edited by T. Fujiwara and Y. Ishii (Elsevier, Amsterdam, 2008), p. 75.

⁶A. P. Tsai, *Sci. Tech. Adv. Mater.* **9**, 013008 (2008).

⁷H. Takakura, C. P. Gómez, A. Yamamoto, M. de Boissieu, and A. P. Tsai, *Nat. Mater.* **6**, 58 (2007).

⁸N. Fujita and K. Niizeki, *Philos. Mag.* **88**, 1913 (2008).

⁹For a review, see J. Flouquet and H. Harima, e-print [arXiv:0910.3110v2](https://arxiv.org/abs/0910.3110v2).

¹⁰S. Wada and A. Yamamoto, *Physica B: Condens. Matt.* **403**, 1202 (2008).

¹¹C. P. Gómez and H. Takakura (unpublished).

¹²T. Watanuki, A. Machida, T. Ikeda, A. Ohmura, H. Kaneko, K. Aoki, T. J. Sato, and A. P. Tsai, *Philos. Mag.* **87**, 2905 (2007).

¹³C. Dallera, E. Annese, J.-P. Rueff, A. Palenzona, G. Vankó, L. Braicovich, A. Shukla, and M. Grioni, *Phys. Rev. B* **68**, 245114 (2003).

¹⁴T. Watanuki, T. J. Sato, and A. P. Tsai, *J. Phys.: Conf. Ser.* **215**, 012019 (2010).

¹⁵G. Krauss, Q. F. Gu, S. Katrych, and W. Steurer, *J. Phys. Condens. Matter* **19**, 116203 (2007).

¹⁶D. A. Young, *Phase Diagrams of the Elements* (University of California Press, Berkeley, CA, 1991), p. 273.

¹⁷A. V. Goltsev and M. M. Abd-Elmeguid, *J. Phys. Condens. Matter* **17**, 813 (2005).

¹⁸For a review, see J.-P. Rueff and A. Shukla, *Rev. Mod. Phys.* **82**, 847 (2010).

¹⁹A. Palenzona and S. Cirafici, *High Temp. High Press.* **17**, 547 (1985).

²⁰R. Tamura, Y. Murao, S. Kishino, S. Takeuchi, K. Tokiwa, and T. Watanabe, *Mater. Sci. Eng. A* **375–377**, 1002 (2004).

²¹S. K. Dhar, A. Palenzona, P. Manfrinetti, and S. M. Pattalwar, *J. Phys. Condens. Matter* **14**, 517 (2002). The value was converted by applying the definition of “mol” as an atomic mole.

²²A. L. Pope, T. M. Tritt, R. Gagnon, and J. Strom-Olsen, *Appl. Phys. Lett.* **79**, 2345 (2001).

²³For a review, see Ö. Rapp, in *Physical Properties of Quasicrystals*, edited by Z. M. Stadnik (Springer, Berlin, 1999), p. 127.

²⁴S. Nakatsuji, K. Kuga, Y. Machida, T. Tayama, T. Sakakibara, Y. Karakai, H. Ishimoto, S. Yonezawa, Y. Maeno, E. Pearson, G. G. Lonzarich, L. Balicas, H. Lee, and A. Fisk, *Nat. Phys.* **4**, 603 (2008).

²⁵M. Okawa, M. Matsunami, K. Ishizaka, R. Eguchi, M. Taguchi, A. Chainani, Y. Takata, M. Yabashi, K. Tamasaku, Y. Nishino, T. Ishikawa, K. Kuga, N. Horie, S. Nakatsuji, and S. Shin, *Phys. Rev. Lett.* **104**, 247201 (2010).